

Pen-on-Paper Approach Toward the Design of Universal Surface Enhanced Raman Scattering Substrates

Lakshminarayana Polavarapu,* Andrea La Porta, Sergey M. Novikov,
Marc Coronado-Puchau, and Luis M. Liz-Marzán*

The translation of a technology from the laboratory into the real world should meet the demand of economic viability and operational simplicity. Inspired by recent advances in conductive ink pens for electronic devices on paper, we present a “pen-on-paper” approach for making surface enhanced Raman scattering (SERS) substrates. Through this approach, no professional training is required to create SERS arrays on paper using an ordinary fountain pen filled with plasmonic inks comprising metal nanoparticles of arbitrary shape and size. We demonstrate the use of plasmonic inks made of gold nanospheres, silver nanospheres and gold nanorods, to write SERS arrays that can be used with various excitation wavelengths. The strong SERS activity of these features allowed us to reach detection limits down to 10 attomoles of dye molecules in a sample volume of 10 μL , depending on the excitation wavelength, dye molecule and type of nanoparticles. Furthermore, such simple substrates were applied to pesticide detection down to 20 ppb. This universal approach offers portable, cost effective fabrication of efficient SERS substrates at the point of care. This approach should bring SERS closer to the real world through ink cartridges to be fixed to a pen to create plasmonic sensors at will.

1. Introduction

What if we could create our own SERS substrates at the point care for preliminary assessment of a suspected disease or to detect specific chemical species? This challenge is to be addressed to transform the SERS technology and bring it closer to the real world.^[1,2] The recent developments on smart

phones coupled with spectrometers are encouraging towards portable detection based on Raman signals.^[3–5] Over the past decade or so, surface enhanced Raman scattering (SERS) has emerged as one of the most attractive and powerful spectroscopic techniques for label-free ultrasensitive (down to single molecule level) detection of chemical and biological species, because of its ability to provide a spectroscopic fingerprint of each molecule.^[6–9] SERS has largely profited from recent advances in the wet chemical and lithography-based preparation of plasmonic nanostructures with tunable optical properties.^[10–13] SERS is expected to play a vital role in various fields, such as medical diagnostics, environmental and security applications in the near future. However, the transformation of this technology into real world applications has been largely hindered by problems mainly associated with reproducibility and complexity in the preparation of SERS substrates. SERS substrates have been prepared by both top-down and bottom-up approaches, including electron beam lithography, colloidal lithography, chemical vapor deposition, chemical attachment of nanoparticles to glass substrates

Dr. L. Polavarapu, A. La Porta, Dr. S. M. Novikov,
M. Coronado-Puchau, Prof. L. M. Liz-Marzán
Bionanoplasmonics Laboratory
CIC biomaGUNE
Paseo de Miramón 182, 20009
Donostia – San Sebastian, Spain
E-mail: lpolavarapu@cicbiomagune.es; llizmarzan@cicbiomagune.es
Prof. L. M. Liz-Marzán
Ikerbasque, Basque Foundation for Science
48011 Bilbao, Spain
DOI: 10.1002/sml.201400438



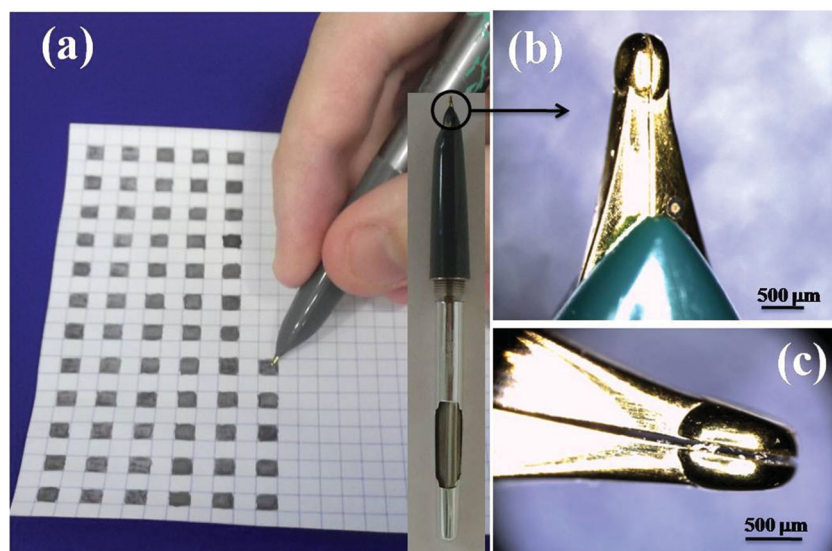


Figure 1. (a) Photograph of a fountain pen loaded with a plasmonic nanoparticle ink and writing SERS substrates on paper (the inset shows the inner part of the pen). (b,c) Optical microscopy images of the nib at two different magnifications.

and self-assembly.^[13–16] Substrates prepared by means of the above methods exhibit excellent performance, but large scale preparation invariably leads to laborious and relatively expensive processes, which often require sophisticated instrumental facilities.

To overcome such problems associated with conventional SERS substrates, much attention has been recently paid towards paper based SERS substrates. Paper is inexpensive, flexible, biodegradable, disposable and light weight, samples can be wicked by capillary forces and it is widely used in our daily life.^[1,17–26] A great deal of research has been carried out to impregnate plasmonic nanoparticles into paper through various processes such as dip coating, inkjet printing, screen printing and physical vapor deposition.^[1,17–25] For instance, Srikanth and co-workers reported SERS paper substrates impregnated with gold nanorods by dip coating.^[17,21,27] However, the process required dipping the paper into a concentrated nanoparticles solution for two days.^[17,25] Yu et al.^[19,22] reported inkjet printing of SERS arrays on hydrophobized cellulose paper. Batch fabrication of SERS substrates by screen printing has been reported by Lu et al.^[24] However, all these processes require some kind of instrumentation. In order to fabricate viable and economical SERS substrates, the whole process should be rapid, simple and close to the real world. Can we make our own SERS substrates without any kind of instrumentation? Recently, Russo et al.^[28] reported a pen that can be used to write flexible electronic devices on paper. Various other types of conductive nanoparticle ink pens are available in the market. Can we use a similar approach to fabricate SERS substrates immediately before sample analysis?

This idea motivated us to investigate a pen-on-paper (POP) approach for the fabrication of SERS substrates (see Supporting Movie S1). This is a simple way of making efficient SERS substrates by directly writing on paper

using a pen filled with plasmonic nanoparticle inks. We studied the SERS properties of plasmonic paper substrates prepared by using three different types of nanoparticles (Au nanospheres, Au nanorods and Ag nanospheres), at three different excitation wavelengths. Our substrates exhibit high SERS activity at all three excitation wavelengths, but the SERS efficiency varies depending on the shape and composition of the metal nanoparticles, as expected. In principle, plasmonic nanoparticle aqueous colloids of any shape or size that are stable at relatively high concentrations could be used as inks and one can select the type of ink depending on the required excitation wavelength. In addition, these substrates exhibit rather high uniformity across different substrates made from the same ink, as well as long term stability, and they outperform commercially available SERS substrates. Finally, we demonstrate

the application of such substrates for the detection of a pesticide down to 20 ppb.

2. Results and Discussion

In the present POP approach, an ordinary fountain pen with a cost of $\approx 0.5\$$ was chosen for writing SERS substrates on paper, as shown in **Figure 1**. Fountain pens contain a reservoir of aqueous ink and the pen can draw the ink from the reservoir and dispense it on paper through the nib (Figure 1b,c), via a combination of capillary action and gravity. Depending on the fountain pen model, ink can be filled into the reservoir through the nib by suction or by filling the ink directly into a removable reservoir, like pre-filled ink cartridges. In the present case, the pen had a 2 mL reservoir that was partially filled with ink by suction through the nib (see **Movie S1**). Figure 1a–c shows a photograph (Figure 1a) and optical microscopy images (Figure 1b,c) of a fountain pen with a nib diameter of $\approx 125\ \mu\text{m}$ that is filled with a nanoparticle ink. Since paper is made of organic compounds, it is important that they exhibit weak Raman cross sections. Therefore, we measured the Raman spectra of paper ($80\ \text{g/m}^2$ white colour A4 photocopy paper) at three different excitation wavelengths and found that no Raman bands were detected within the spectral region where most molecules of interest are Raman active (Figure S1). Interestingly, unlike filter paper, A4 photocopy paper exhibits a certain degree of hydrophobicity, which helps to concentrate the sample on the SERS active area alone, rather than spreading it all over the paper by capillarity (Figure S2). This is interesting because it allows us to avoid a hydrophobizing step by chemical functionalization, which is typically necessary to concentrate the analyte molecules at a small SERS sensing area to obtain a higher efficiency.^[22]

An essential part of this POP approach is the plasmonic nanoparticle ink, which must readily flow through the nib during writing, be stable at higher nanoparticle concentrations and be highly SERS active upon writing on paper. The SERS activity of plasmonic nanoparticles depends on their size, shape and the type of metal, which govern their surface plasmon resonance properties. Among various metal nanoparticles, spherical gold nanoparticles are one of the simplest systems in terms of preparation and size tunability. Thus, we first synthesized spherical gold nanoparticles within a wide size range (≈ 15 – 120 nm) and studied their size-dependent SERS properties using crystal violet as Raman probe, so as to select the most appropriate particle size for the nanoparticles ink in the POP approach (Figures S3, S4). As particle size increases, the UV-vis spectra were found to become broader and the localized surface plasmon resonance (LSPR) bands exhibit a gradual red shift, leading to effective coupling with the 633 nm excitation laser. As a consequence, the SERS efficiency increases with nanoparticle size up to ≈ 95 – 100 nm and then it remains constant or decreases with further increase of particle size (Figure S4). Additionally, particles with sizes above 100 nm exhibit poor colloidal stability in water and tend to settle down on the bottom of the container. On the basis of these results, we selected particles with an average diameter of ≈ 95 nm (Figure 2a) as nanoparticle ink to test the SERS arrays prepared by the POP approach.

It is known from previous studies that both anisotropic gold nanostructures and silver nanoparticles exhibit higher SERS activity than gold spheres. Thus, we also prepared Au NR and Ag NP inks and tested the SERS activity of substrates prepared from them. Unlike Au NPs, the size tunability of Ag NPs by the citrate reduction method is limited as they often produce polydisperse Ag NPs. We synthesized quasi-spherical Ag NPs of sizes ranging between 50 and 80 nm, as shown in Figure 2g (see Figure S5 for the corresponding extinction spectrum). Au NRs with an aspect ratio of 3.6 (50 nm long, 14 nm thick) were prepared, which exhibit a longitudinal LSPR maximum at 665 nm (see Figure 2e for TEM and Figure S6 for the corresponding extinction spectrum), which

is close to the excitation wavelength of 633 nm. In general, as prepared nanoparticles of any size or shape are not sufficiently concentrated to be used as inks and we thus increased the concentration by centrifugation. Moreover, excess surfactant present in the colloid should be removed to allow the analyte molecules to reach the nanoparticles surface and achieve higher SERS activity, while preserving the particles stability after purification. We used centrifugation to purify and concentrate the nanoparticles to 3 mg/mL. Details of the preparation of nanoparticle inks are provided in the experimental section.

Figure 2(a,e,g) shows TEM images of Au NPs, Au NRs and Ag NPs, together with representative photographs of the corresponding inks. Au NPs and Au NRs are uniform in size, whereas Ag NPs exhibit polydispersity including a significant amount of high aspect ratio Ag nanorods. Figure 2b shows an SEM image of the paper comprising a network of micron scale (10–20 μm) cellulose fibers. The three different inks were filled into three fountain pens to write SERS arrays of the corresponding NPs (note that any standard fountain pen can be used). The inks freely flow through the nib and are deposited on paper by writing so that the morphology of the SERS substrate can be easily controlled (Movie S1). The minimum size of the SERS spot that can be created is determined by the nib dimension (125 μm in the present case). In this approach, a tiny volume of ink can be used to create large scale SERS arrays. For example, 0.2 mL of ink was used to create 15×15 SERS spot arrays with a spot area of 0.9 cm^2 . SEM images of the SERS substrates prepared using three different inks via the POP approach are presented in Figure 2(d,f,g). These images show that the nanoparticles are densely packed and adsorbed onto the surface of cellulose fibers, so they are expected to produce intense SERS signals.

Another important factor that should be considered in the design of SERS substrates is their stability and robustness. In most early studies, the design was based on the immobilization of plasmonic nanoparticles on glass substrates, either by chemical or electrostatic interactions. However, such substrates were found to be marginally stable and the particles

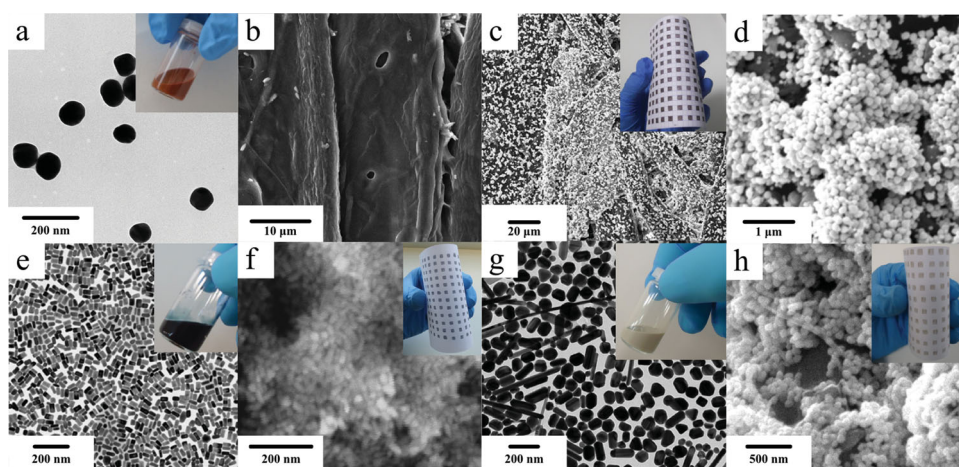


Figure 2. (a) TEM image of Au nanoparticles and photograph of a representative ink. (b,c,d) SEM images of the paper before (b) and after (c,d at different magnifications) writing the SERS arrays. The inset in c shows an optical photograph of SERS-active arrays created by the POP approach. (e,g) TEM images of Au nanorods (e) and silver nanoparticles (g), and photographs of representative inks. (f,h) SEM images of SERS substrates prepared by using Au nanorods (f) and Ag nanoparticles (h) inks and photographs of the corresponding SERS arrays.

may detach from the surface during use. We examined the adhesion between metal NPs and paper substrate, in comparison with conventional SERS glass substrates, through the so-called scotch tape test.^[29] For this test, a piece of scotch tape was pressed on the corresponding substrate and slowly pulled off (Figure S7). When this process was applied to Au nanoparticles attached to a 3-aminopropyl-trimethoxysilane (APTMS) modified glass substrate,^[30] this conventional SERS substrate was found to lift off. However, nanoparticles immobilized on paper did not come off with the scotch tape, indicating strong adhesion to the paper substrate (Figure S7). In addition, these substrates are stable in water, as indicated by the invariance of the patterns after dipping in water and subsequent drying (Figure S8).

The SERS performance of three different substrates was characterized by drying on them a 10 μ L droplet of malachite green (MG) as Raman active probe. MG is an organic dye, which has an effective fungicide effect that is widely used in fish farms, in the aquaculture industry and in freshwater aquaria. However, the use of malachite green is rather controversial due to its genotoxic and carcinogenic nature and it is banned in several countries. It is thus important to detect trace amounts of MG in water.^[31] Figure 3a shows the SERS spectra of malachite green (1 mM) on three substrates under 633 nm laser excitation. It is clear that all three substrates exhibit SERS activity and the spectra clearly show the characteristic Raman peaks of MG: ring C–C stretching (1618 cm^{-1}), N-phenyl stretching (1397 cm^{-1}), ring C–H in-plane bending (1172 cm^{-1}), C–H out-of-plane bending (917 cm^{-1}). From the acquired data, the SERS efficiency of such three substrates is in the order: Ag NPs > Au

NRs > Au NPs, under the present experimental conditions. As expected, Au NRs exhibit higher field enhancement over spherical Au NPs, leading to higher efficiency. However, in the case of Ag NPs substrate, even though they are smaller than the Au NPs, their efficiency is highest. It has been reported that in general Ag NPs exhibit higher SERS efficiency than Au NPs due to their higher extinction cross section.^[32,33] This trend was also observed with other Raman active probes, suggesting that these substrates exhibit high SERS activity irrespective of the type of Raman probe (Figure S9).

Uniformity is another major concern for any SERS substrate. In order to study the uniformity of the SERS substrates prepared by the POP approach, we registered SERS signals from 15 random sites on a single square drawn with Au NRs and the data are depicted in Figure 3b,c. The results indicate that the variation of intensity is within 10–20% (higher variations were rarely observed due to variation of NP density and non uniform drying of analyte at some places). In addition, we also tested the intensity variations from spot to spot within an array (Figure 3d), showing a high reproducibility. These results are remarkable considering the simplicity of preparation, cheapness and robustness of the substrates. Furthermore, the sensitivity of Au NRs and Ag NPs SERS substrates was tested as shown in Figure 3e and 3f, respectively. MG SERS signals are clearly detectable down to 1 nM on Au NRs and 0.1 nM on Ag NPs substrates, which represents 10 and 1 femtomoles of MG molecules, respectively, in 10 μ L of sample volume. The sensitivity of these substrates is similar or even higher than that of substrates prepared by inkjet printing, depending on the type of NP ink.^[22]

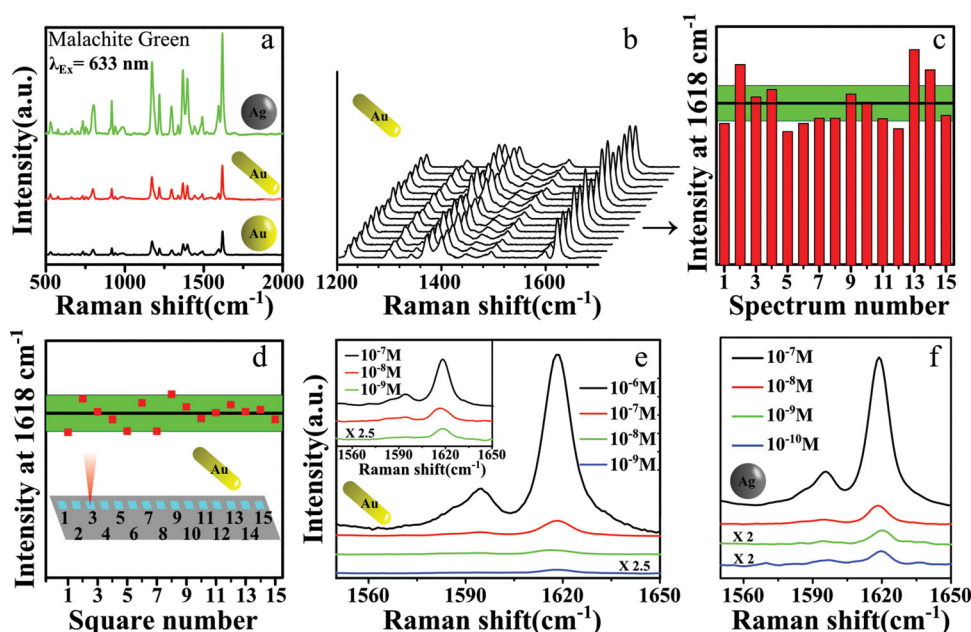


Figure 3. (a) SERS spectra of malachite green (1 μ M) acquired from three different substrates (Au NPs, Au NRs, Ag NPs) prepared by POP approach. (b,c) SERS spectra of malachite green acquired from 15 different spots within a single square drawn on paper substrate with Au NRs ink (a) and the corresponding histogram for the peak intensity at 1618 cm^{-1} (c). (d) Reproducibility of SERS arrays prepared with Au NRs ink. SERS spectra were acquired at 15 different square spots from an array (Inset shows the schematic representation of SERS measurements on a 15 point array). (e) SERS spectra (peak at 1618 cm^{-1}) of different concentrations (10^{-6} to 10^{-9} M) of malachite green on Au NRs substrate (the spectrum obtained at 10^{-9} M was amplified 2.5 fold for clarity). (f) SERS spectra (peak at 1618 cm^{-1}) of different concentrations (10^{-6} to 10^{-10} M) of malachite green on Ag NPs substrate (the spectra obtained at 10^{-9} and 10^{-10} M were amplified 2 fold for clarity). All the SERS spectra were acquired at 633 nm excitation.

Although we have so far shown that SERS substrates can be readily prepared at the point of care by means of the POP approach, an ideal substrate should be stable for long periods of time. Thus, the stability of the substrate was studied by comparing the SERS signals from a freshly prepared Au NRs substrate and the substrate after storage under atmospheric conditions for one month (Figure S10). The results show that both substrates exhibit similar intensity on average, illustrating their long term stability. However it should be mentioned that long term stability might not be possible with all nanoparticle types, particularly with Ag NPs as they tend to oxidize easily when they are transferred from solution onto substrates. In such cases, the preparation of substrates at the point of care is crucial and this approach offers a unique way of preparation. Importantly, all three substrates exhibited higher SERS efficiency than commercial SERS substrates under the same experimental parameters (Figure S11). Most of the results presented above were obtained with an excitation wavelength of 633 nm. For completeness, the SERS activity of the substrates was also studied with 532 and 785 nm laser excitations and the results are depicted in **Figure 4**. We found that all three substrates exhibit SERS activity under 785 nm excitation, which is important in bio-related applications, but Au NPs and Au NRs substrates show poor SERS signals for MG under 532 nm excitation (inset of Figure 4a), due to plasmon damping by coupling to inter-band transitions.^[33,34] However, Ag NP substrates do exhibit

intense SERS activity with 532 nm excitation. We studied the SERS efficiency of Ag NPs substrates with 532 nm excitation for R6G detection, which has been reported for other Ag NP substrates.^[35] Interestingly, our Ag NPs substrates provided extremely high sensitivity down to 10^{-12} M, corresponding to 10 attomoles of R6G molecules in a 10 μ L sample volume. As shown in Figure 4c, the SERS signal intensity gradually decreased with the decrease of R6G concentration, pointing toward the possibility of quantitative analyte determination. The average enhancement factor (EF) of the Ag NPs substrates was calculated using MG and the obtained values are 2×10^5 and 1.5×10^5 at 532 and 785 nm, respectively. These average EFs are similar to those previously reported for some of the conventional SERS substrates^[36] and even with inkjet-printed SERS substrates.^[22]

We finally demonstrate the application of these substrates for the detection of thiabendazole, which is a fungicide and parasiticide. It has been widely used as food preservative and additive, but it is not approved in EU, Australia and New Zealand due to its toxicity at higher doses. **Figure 5a** shows the SERS spectra of thiabendazole (20 ppm) acquired with different excitation wavelengths, illustrating the ability to detect it with any available excitation wavelength. At all excitation wavelengths, the characteristic SERS signals of thiabendazole were registered: skeletal ring stretching modes (1580 cm^{-1} , 1546 cm^{-1}), phenyl ring breathing mode (1010 cm^{-1}), Ag-S bond stretch (782 cm^{-1}) and C-N stretch (1280 cm^{-1}). SERS

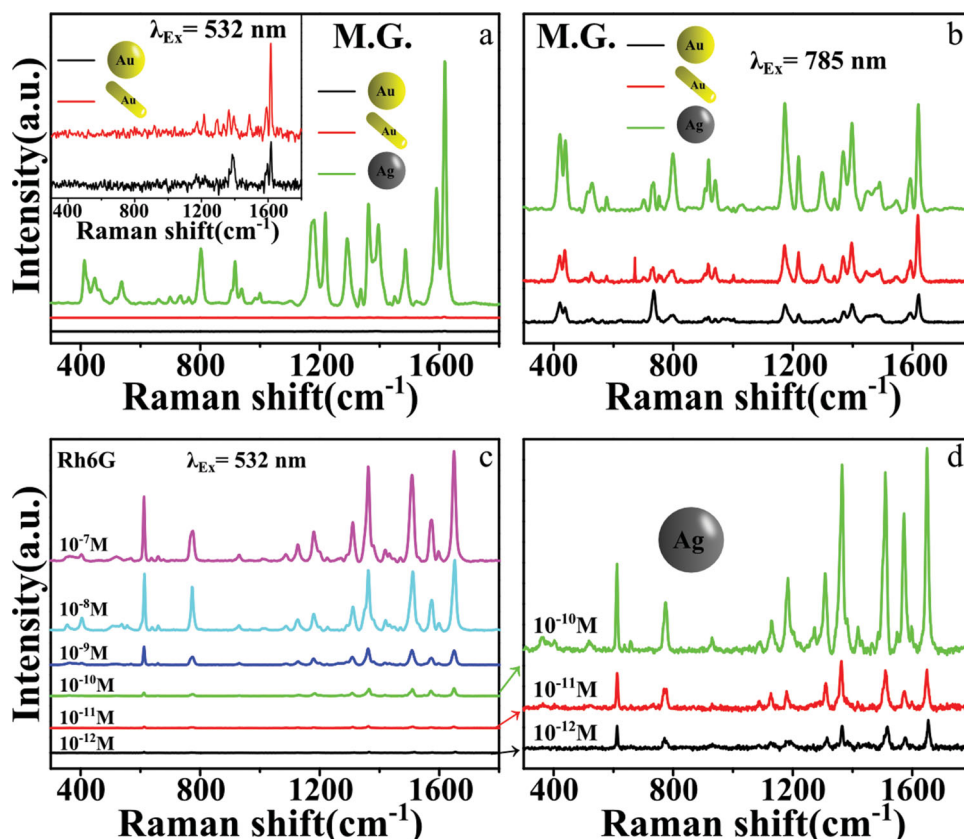


Figure 4. (a, b) SERS spectra of malachite green (1 μ M) collected from three different SERS substrates (Au NPs, Au NRs, Ag NPs) with excitation wavelengths of 532 nm (a) and 785 nm (b). The inset in a shows magnified spectra of MG collected from Au NPs and Au NRs substrates. (c) SERS spectra of R6G at different concentrations (10^{-7} to 10^{-12} M) on Ag NPs substrate with 532 nm excitation. (d) Magnified spectra at low concentrations (10^{-10} – 10^{-12} M).

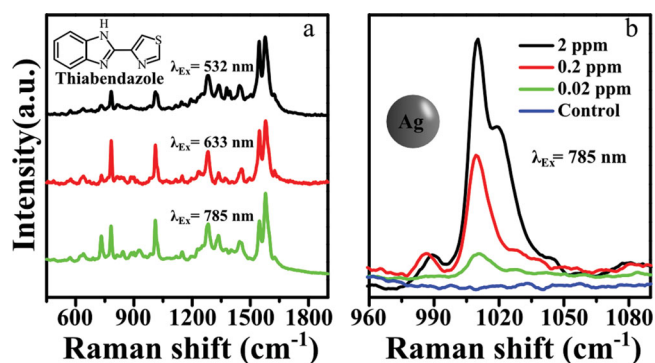


Figure 5. (a) SERS spectra of thiabendazole (20 ppm) on Ag NPs substrate with three different excitation wavelengths of 532, 633 and 785 nm. (b) SERS spectra (peak at 1008 cm^{-1}) of thiabendazole with different concentrations (2, 0.2, 0.02 ppm) on Ag NPs substrate with 785 nm excitation.

analysis of thiabendazole at 785 nm excitation and decreasing concentrations showed a detection sensitivity of 20 ppb in a $10\text{ }\mu\text{L}$ sample volume (Figure 5b).

3. Conclusions

We have demonstrated the application of the pen-on-paper approach, developed in the field of paper electronics, for simple and economically viable design of highly efficient, reproducible, uniform and low-cost SERS substrates. In this approach, a fountain pen filled with plasmonic nanoparticles ink was used to directly write SERS arrays on paper substrates with no need of any professional training. Au NP, Au NR and Ag NP inks were tested for the preparation of efficient SERS substrates, which exhibit highly efficient detection, even down to 10 attomoles of molecules in a sample volume of $10\text{ }\mu\text{L}$, depending on the excitation wavelength, dye molecule and the type of nanoparticles. Such substrates, in particular those containing Ag NPs, exhibit high SERS activity over a broad range of excitation wavelengths. As a practical application, we demonstrated the detection of toxic parasiticide molecules down to 20 ppb in a $10\text{ }\mu\text{L}$ sample volume. Thus, this universal approach is expected to bring the SERS technology closer to real world applications.

4. Experimental Section

Materials: Tetrachloroauric acid ($\text{HAuCl}_4 \cdot 3\text{H}_2\text{O}$), trisodium citrate dihydrate, silver nitrate (AgNO_3), L-ascorbic acid, Rhodamine 6G, crystal violet, and thiabendazole were purchased from Sigma-Aldrich. Cetyltrimethyl ammonium bromide (CTAB) and malachite green were purchased from Fluka. All chemicals were used as received, without further purification. Fountain pens were purchased from a general store in India with a cost of $\approx 0.5\text{ \$}$ per pen. Glassware was washed with aqua regia followed by water. Milli-Q water (Millipore) was used throughout the experiments.

Preparation of Au nanoparticles of different sizes and NPs ink: Citrate-stabilized Au NPs of different sizes were prepared by the kinetically controlled seeded growth method reported by Bastús

et al.^[37] Briefly, Au seeds were first prepared by injecting HAuCl_4 (1 mL, 25 mM) solution to the boiling solution of sodium citrate (150 mL, 2.2 mM). The colour of the solution changes from colourless to pink after 10 min of reaction. In order to grow the obtained seeds into bigger Au NPs, the reaction temperature of the seed solution was first cooled down to $90\text{ }^\circ\text{C}$ immediately after seed formation and then HAuCl_4 solution (1 mL, 25 mM) was added. After 30 min of reaction time, another of HAuCl_4 solution (1 mL, 25 mM) was injected. After the reaction, the sample was diluted by extracting 55 mL of the obtained Au NPs solution and adding water (53 mL) and sodium citrate (2 mL, 60 mM). The obtained colloid was used as seed solution to further increase the Au NPs size. Such process was continued until the Au NPs size reached to 115 nm. From the size dependent SERS measurements, 95 nm NPs were selected to prepare Au NPs ink, which was prepared by concentrating the obtained Au NPs (100 mL) into 1.5 mL by centrifugation for a final concentration of 3 mg/mL.

Preparation of Au nanorod ink: Gold nanorods were prepared by seed mediated growth.^[38] Seed solution was prepared by adding ice-cold NaBH_4 solution (0.3 mL, 10 mM) to a mixture of CTAB (4.7 mL, 0.1 M) and HAuCl_4 (25 μL , 0.05 M) aqueous solution under vigorous stirring at room temperature. Upon NaBH_4 addition, the solution colour changes from pale yellow to brown, indicating the formation of small seed particles. Nanorods were grown by adding 0.36 mL of seed solution to a growth solution (prepared by mixing CTAB (150 mL, 0.1M), HAuCl_4 (1.5 mL, 0.05 M), AgNO_3 (0.225 mL, 0.01 M), ascorbic acid (0.12 mL, 0.1M)). The solution colour changes from colourless to blue after the addition of seed solution to the grown solution. The obtained solution was centrifuged twice and redispersed in water (2 mL) to obtain Au NR ink (3 mg/mL). The final concentration slightly varied from batch to batch depending on the purification step, however it can be easily adjusted by either diluting or concentrating the obtained NPs solution.

Preparation of Ag nanoparticle ink: The Ag NPs were synthesized according to the Lee and Meisel method.^[39] Briefly, trisodium citrate solution (4.5 mL, 1.00 wt%) was added to the boiling solution containing AgNO_3 (200 mL, 42 mg) of water under vigorous stirring. The reaction was boiled for another 1 hr and then cooled to room temperature. The obtained Ag nanoparticles in water (200 mL) were centrifuged at 7000 rpm for 20 min and then redispersed in water (2 mL) to obtain Ag NP ink (3 mg/mL).

Characterization: The optical properties of nanoparticle solutions were recorded using an Agilent 8453 UV-Vis spectrophotometer. TEM images were obtained using a JEOL JEM 1400 Plus microscope operating at an acceleration voltage of 100 kV. For SEM measurements, nanoparticles impregnated papers were first coated with a layer of Ti-Au ($\approx 3\text{ nm}$) to make their surface partially conductive to minimize charging effects. SEM images of Au and Ag NPs were obtained using SEM (JEOL 6490LV) and the SEM images of Au NRs were obtained using ESEM Quanta250 FEG (FEI company, Netherlands). Optical photographs of a pen nib were obtained with an optical microscope (Leica Microsystems).

Size dependent SERS study of Au NPs suspensions: Size dependent SERS properties of Au NPs were measured by adding crystal violet solution (20 μL , 10 μM) to Au NPs (1 mL, 0.02 nM nanoparticle concentration) of different sizes and then the average SERS signals were recorded from the NPs suspensions using a micro-Renishaw InVia Reflex system equipped with Peltier

charge-coupled device (CCD) detectors with the excitation wavelength of 633 nm.

SERS measurements on NPs substrates prepared by POP approach: SERS substrates were prepared by direct writing of SERS arrays on paper and each spot of the array is a square with an area of $0.3 \times 0.3 \text{ cm}^2$. SERS measurements were performed using the same Raman system mentioned above. For SERS characterisation, a 10 μL of analyte was dropped onto a NPs impregnated paper substrate having dimensions of $0.3 \times 0.3 \text{ cm}^2$ and then dried in an oven at 60 °C for 5 minutes. The signals from each sample were collected for 10 s using a 100 \times objective with three different excitation wavelengths of 532, 633 and 785 nm. The laser beam was focused on the nanoparticle clusters by selecting an area through the optical microscope connected to the Renishaw Raman spectrometer. Importantly, the focus of the laser beam was adjusted to maximum SERS signal at each point as the microscopic organization of fibers is not flat.

Supporting Information

Supporting Information is available from the Wiley Online Library or from the author.

Acknowledgements

This work was funded by the European Research Council (ERC Advanced Grant #267867 Plasmaquo). The authors thank Judith Langer for helpful discussions. Authors thank Dr. Yuri Rakovich at Materials Physics Center (CFM) in San Sebastian for providing us with the commercial SERS substrate.

- [1] L. Polavarapu, L. M. Liz-Marzan, *Phys. Chem. Chem. Phys.* **2013**, *15*, 5288–5300.
- [2] J. F. Betz, W. W. Yu, Y. Cheng, I. M. White, G. W. Rubloff, *Phys. Chem. Chem. Phys.* **2014**, *16*, 2224–2239.
- [3] Q. Wei, H. Qi, W. Luo, D. Tseng, S. J. Ki, Z. Wan, Z. Göröcs, L. A. Bentolila, T.-T. Wu, R. Sun, A. Ozcan, *ACS Nano* **2013**, *7*, 9147–9155.
- [4] S. Ayas, A. Cupallari, O. O. Ekiz, Y. Kaya, A. Dana, *ACS Photonics* **2014**, *1*, 17–26.
- [5] S. Khatua, M. Orrit, *ACS Nano* **2013**, *7*, 8340–8343.
- [6] R. A. Alvarez-Puebla, L. M. Liz-Marzán, *Small* **2010**, *6*, 604–610.
- [7] J. N. Anker, W. P. Hall, O. Lyandres, N. C. Shah, J. Zhao, R. P. Van Duyne, *Nat. Mater.* **2008**, *7*, 442–453.
- [8] Y. W. C. Cao, R. C. Jin, C. A. Mirkin, *Science* **2002**, *297*, 1536–1540.
- [9] S. M. Nie, S. R. Emory, *Science* **1997**, *275*, 1102–1106.
- [10] M. Grzelczak, L. M. Liz-Marzán, *Langmuir* **2013**, *29*, 4652–4663.
- [11] J. P. Camden, J. A. Dieringer, J. Zhao, R. P. Van Duyne, *Acc. Chem. Res.* **2008**, *41*, 1653–1661.
- [12] S. E. Lohse, C. J. Murphy, *Chem. Mater.* **2013**, *25*, 1250–1261.
- [13] C. L. Haynes, R. P. Van Duyne, *J. Phys. Chem. B* **2001**, *105*, 5599–5611.
- [14] M. Fan, G. F. S. Andrade, A. G. Brolo, *Anal. Chim. Acta* **2011**, *693*, 7–25.
- [15] S. L. Kleinman, R. R. Frontiera, A.-I. Henry, J. A. Dieringer, R. P. Van Duyne, *Phys. Chem. Chem. Phys.* **2013**, *15*, 21–36.
- [16] R. A. Alvarez-Puebla, A. Agarwal, P. Manna, B. P. Khanal, P. Aldeanueva-Potel, E. Carbo-Argibay, N. Pazos-Perez, L. Vigderman, E. R. Zubarev, N. A. Kotov, L. M. Liz-Marzan, *Proc. Natl. Acad. Sci. U. S. A.* **2011**, *108*, 8157–8161.
- [17] C. H. Lee, L. M. Tian, S. Singamaneni, *ACS Appl. Mater. Interf.* **2010**, *2*, 3429–3435.
- [18] W. W. Yu, I. M. White, *Analyst* **2013**, *138*, 3679–3686.
- [19] W. W. Yu, I. M. White, *Analyst* **2013**, *138*, 1020–1025.
- [20] M. L. Cheng, B. C. Tsai, J. Yang, *Anal. Chim. Acta* **2011**, *708*, 89–96.
- [21] C. H. Lee, M. E. Hankus, L. Tian, P. M. Pellegrino, S. Singamaneni, *Anal. Chem.* **2011**, *83*, 8953–8958.
- [22] W. W. Yu, I. M. White, *Anal. Chem.* **2010**, *82*, 9626–9630.
- [23] R. Zhang, B.-B. Xu, X.-Q. Liu, Y.-L. Zhang, Y. Xu, Q.-D. Chen, H.-B. Sun, *Chem. Commun.* **2012**, *48*, 5913–5915.
- [24] L.-L. Qu, D.-W. Li, J.-Q. Xue, W.-L. Zhai, J. S. Fossey, Y.-T. Long, *Lab Chip* **2012**, *12*, 876–881.
- [25] Y. H. Ngo, D. Li, G. P. Simon, G. Garnier, *Langmuir* **2012**, *28*, 8782–8790.
- [26] E. W. Nery, L. T. Kubota, *Anal. Bioanal. Chem.* **2013**, *405*, 7573–7595.
- [27] A. Abbas, A. Brimer, J. M. Slocik, L. M. Tian, R. R. Naik, S. Singamaneni, *Anal. Chem.* **2013**, *85*, 3977–3983.
- [28] A. Russo, B. Y. Ahn, J. J. Adams, E. B. Duoss, J. T. Bernhard, J. A. Lewis, *Adv. Mater.* **2011**, *23*, 3426–3430.
- [29] K. S. Lim, W.-J. Chang, Y.-M. Koo, R. Bashir, *Lab Chip* **2006**, *6*, 578–780.
- [30] Q. Su, X. Ma, J. Dong, C. Jiang, W. Qian, *ACS Appl. Mater. Interf.* **2011**, *3*, 1873–1879.
- [31] S. Lee, J. Choi, L. Chen, B. Park, J. B. Kyong, G. H. Seong, J. Choo, Y. Lee, K. H. Shin, E. K. Lee, S. W. Joo, K. H. Lee, *Anal. Chim. Acta* **2007**, *590*, 139–144.
- [32] S. Gómez-Graña, J. Pérez-Juste, R. A. Alvarez-Puebla, A. Guerrero-Martínez, L. M. Liz-Marzán, *Adv. Opt. Mater.* **2013**, *1*, 477–481.
- [33] L. Polavarapu, K. K. Manga, K. Yu, P. K. Ang, H. D. Cao, J. Balapanuru, K. P. Loh, Q.-H. Xu, *Nanoscale* **2011**, *3*, 2268–2274.
- [34] M. Rycenga, K. K. Hou, C. M. Cobley, A. G. Schwartz, P. H. C. Camargo, Y. Xia, *Phys. Chem. Chem. Phys.* **2009**, *11*, 5903–5908.
- [35] K. L. Wustholz, C. L. Brosseau, F. Casadio, R. P. Van Duyne, *Phys. Chem. Chem. Phys.* **2009**, *11*, 7350–7359.
- [36] L. Osinkina, T. Lohmüller, F. Jäckel, J. Feldmann, *J. Phys. Chem. C* **2013**, *117*, 22198–22202.
- [37] N. G. Bastús, J. Comenge, V. F. Puntes, *Langmuir* **2011**, *27*, 11098–11105.
- [38] B. Nikoobakht, M. A. El-Sayed, *Chem. Mater.* **2003**, *15*, 1957–1962.
- [39] P. C. Lee, D. Meisel, *J. Phys. Chem.* **1982**, *86*, 3391–3395.

Received: February 17, 2014

Revised: March 26, 2014

Published online: May 2, 2014